The Apolar Distal Histidine Mutant (His69→Val) of the Homodimeric *Scapharca* Hemoglobin Is in an *R*-like Conformation†

Laura Guarrera,‡ Gianni Colotti,‡ Alberto Boffi,‡ Emilia Chiancone,*,‡ Tapan Kanti Das,§ Denis L. Rousseau,§ and Quentin H. Gibson||

CNR Center of Molecular Biology, Department of Biochemical Sciences, University "La Sapienza", P.le A.Moro 5, 00185 Rome, Italy, Department of Physiology and Biophysics, Albert Einstein College of Medicine, Bronx, New York 10461, and Department of Biochemistry and Cell Biology, Rice University, 6100 Main Street, Houston, Texas 77005

Received September 25, 1997; Revised Manuscript Received December 29, 1997

ABSTRACT: The effect of the apolar mutation of the distal histidine (His69→Val) has been studied in the cooperative homodimeric hemoglobin from the mollusc *Scapharca inaequivalvis*. Absorption, circular dichroism, and resonance Raman spectroscopy point to a more symmetric heme structure of the deoxy derivative, which is indicative of an *R*-like conformation of the deoxy heme. Resonance Raman spectroscopy also brings out alterations in the geometry and interactions of the bound CO molecule. The iron−carbon stretching frequency is decreased by about 30 cm^{-1} with respect to the native protein, while the diatomic ligand stretching frequency is increased by about the same degree. Consistent with the structural changes, the ligand binding properties are significantly altered. In the mutant the overall rate and the affinity for CO binding are increased about 100-fold with respect to the native protein, and cooperativity is abolished. In addition, the amplitude and the rate of the geminate rebinding process increase significantly. This finding may be correlated to the longer average residence time of the photolyzed CO molecule within the heme pocket of the H69V mutant, as indicated by molecular dynamics simulations.

The structural basis for the control of ligand binding in hemoproteins has been investigated extensively through site-directed mutagenesis of the amino acid residues in the distal side of the heme pocket. In myoglobins and hemoglobins, several key residues have been identified which contribute to the regulation of oxygen affinity and to the discrimination between oxygen and carbon monoxide for binding to the heme iron. Among these residues, the distal His (E7) plays a major role as it stabilizes the bound oxygen through hydrogen bond donation and provides an effective barrier for the binding of the CO molecule by exerting steric hindrance on bound CO (*1*).

In myoglobins (Mb),[1] mutations of the distal histidine always lead to dramatic changes in the thermodynamic and kinetic properties of the ligand binding reactions. In particular, apolar substitutions result in an increase in CO affinity paralleled by a large reduction (10−100-fold) in O_2 affinity which is due mainly to an increased rate of ligand release (*2*). Oxygen affinity would decrease even further were it not that the bimolecular kinetics of ligand binding is also influenced by the diffusional barrier offered by the water molecule bound to the Nϵ of the distal histidine. In apolar E7 mutants, this water molecule is absent and bimolecular ligand binding is 5−20-fold faster (*2*). The intrinsic iron−ligand bond strength apparently makes only a minor contribution in determining the overall free energy of the binding process. Thus, Li et al. (*3*) have reported a correlation between the CO affinity and the diatomic ligand stretching frequency determined by FTIR in polar and apolar mutants. On the other hand, several authors found an inverse correlation between the Fe−CO stretching frequency and affinity using RR spectroscopy (*3*−*5*).

In human hemoglobin (HbA), apolar E7 mutants have been relatively little studied. The α chain mutants are unstable, and βE7Phe is the only β chain mutant investigated. The HbA−βE7Phe ligand binding properties have been rationalized by assuming that the mutation freezes the protein in the R-state without affecting the intrinsic ligand binding parameters significantly (*6*).

In the present paper, the apolar mutant of the distal histidine (His69→Val) of the homodimeric, cooperative hemoglobin from the mollusc *Scapharca inaequivalvis* (HbI) has been characterized. HbI displays a unique structural basis for cooperative ligand binding in that the two hemes face each other across the intersubunit contact (*7*−*10*). As a consequence of this unusual structural linkage, cooperativity is accompanied by major tertiary changes in the heme environment with only minor rearrangements of the quaternary structure. Upon ligand binding, Phe97, which is in contact with the proximal His in the deoxy state, is extruded into the subunit interface, thus allowing the sinking of the

† This work was supported in part by Research Grant GM54806 (D.L.R.) from the National Institutes of Health and by grants 40% and 60% from MURST to E.C., and by United States Public Health Services Grant GM14276 (Q.H.G.).

‡ University "La Sapienza".

§ Albert Einstein College of Medicine.

|| Rice University.

[1] Abbreviations: Mb, myoglobin; FTIR, Fourier transform infrared spectroscopy; RR, resonance Raman; HbA, human hemoglobin; HbI, dimeric *Scapharca inaequivalvis* hemoglobin; HbI(H69V), dimeric *S. inaequivalvis* hemoglobin mutant in position His69→Val; HbI(T72V), dimeric *S. inaequivalvis* hemoglobin mutant in position Thr72→Val; MD, molecular dynamics.

S0006-2960(97)02380-5 CCC: $15.00
Published on Web 04/01/1998

hemes into the heme pocket. The concomitant changes in the geometry of the heme peripheral substituents permit the transfer of information to the contralateral subunit. The proximal His plays only a minor role when compared with vertebrate hemoglobins (*9*, *11*). The H69V substitution has a dramatic effect on the functional properties of HbI, as it increases the affinity for CO significantly, much more than in the corresponding Mb mutants (*1*), and abolishes cooperativity. These effects have been ascribed to a structural rearrangement which leads to an R-like deoxy conformation characterized by a more symmetric heme coordination geometry.

MATERIALS AND METHODS

Mutagenesis. A single mutation, H69V, was obtained by cassette mutagenesis using the unique *Hind*III and *Pst*I restriction sites of the HbI expression vector (*12*,*13*). Expression of the mutant in *Escherichia coli* and protein purification were carried out as described for recombinant wild-type HbI (*13*).

Absorption and Circular Dichroism Spectra. Absorption spectra of native HbI and HbI(H69V) were measured in the range 380−700 nm, using a Cary 3 spectrophotometer (Varian, Mulgrave, Victoria, Australia). Circular dichroism spectra were recorded in the region between 380 and 480 nm, with a Jasco J 710 spectropolarimeter equipped with a Jasco J700 processor (Jasco, Tokyo, Japan). The measurements were carried out in 0.1 M phosphate buffer, pH 7.0, at 20 °C and at a protein concentration of 8×10^{-6} M. Deoxygenated HbI(H69V) was prepared from a protein solution in which the bound CO was removed by oxidation with a slight excess of potassium ferricyanide. The excess of oxidizing agent was eliminated with a G-25 column. The oxidized mutant was transferred to a tonometer; after equilibration of the solution with pure nitrogen, dithionite was added to achieve complete deoxygenation. Deoxygenated native HbI was obtained by adding a few grains of sodium dithionite to the oxygenated solution.

CO Binding and Dissociation. Carbon monoxide binding experiments were carried out on an Applied Photophysics (Leatherhead, U.K.) stopped flow apparatus by mixing the reduced protein in the presence of 10 mM dithionite with buffer equilibrated with varying CO concentrations. The rate of CO dissociation from the carbon monoxy derivative was measured by mixing the protein solutions (4 μM heme, equilibrated with 10 μM CO) with microperoxidase (16 μM heme) and following the spectral changes in the 400−450 nm region with a Hewlett-Packard 8452A diode array spectrophotometer (*14*). All experiments were carried out at 20 °C in 0.1 M phosphate buffer at pH 7.0.

Laser Photolysis. Measurements of the bimolecular reaction rate with CO by flash photolysis used a solution about 50 μM in heme. The 9-ns, 23-mJ flash at 532 nm came from a Q-switched YAG laser (Continuum Inc., Santa Clara, CA). The beam was telescoped to 2 mm diameter and was collinear with the observation beam, taken from a 75 W Xe arc. The flash gave 50% removal of CO when attenuated some 150-fold. Absorbance excursions were recorded with a monochromator (Spex, *f*/4, 250 mm) and photomultiplier. The output of the multiplier was amplified and transferred to a 1 μs conversion time 12 bit A/D board (Metrabyte Corp., Taunton, MA, model DAS 50) collecting 1024 points for each flash and 50−500 flashes for each record. Nanosecond data were collected with the same optical train. The Xe arc lamp was pulsed during observation using a 4-element lumped parameter transmission line (*15*). This brightened the arc about 200 times for about 50 μs. Data were recorded with a fast photomultiplier (Hamamatsu R1219) coupled directly to a Tektronix 7104 oscilloscope and a CCD camera.

Resonance Raman. Samples for resonance Raman measurements were prepared in 100 mM phosphate buffer, pH 7.4, at a protein concentration of 40 μM. The samples were placed in spinning cylindrical cells of 2 mm light path in a N_2 atmosphere. Incident laser frequencies of 420 (tunable frequency-doubled output from a Ti−Sapphire crystal pumped by an Ar-ion laser, Spectra Physics), 441.6 (He−Cd laser, Liconix), and 413.1 (Kr-ion laser, Spectra Physics) nm were used in resonance Raman measurements of the CO and deoxy derivatives. The Raman scattered light was dispersed through a polychromator (Spex, Metuchen, NJ) equipped with a 1200 grooves/mm grating and detected by a liquid nitrogen-cooled CCD camera (Princeton Instruments, Princeton, NJ). A holographic notch filter (Kaiser, Ann Arbor, MI) was used to remove the laser scattering. Typically, several 2-min spectra were recorded and averaged after removal of cosmic ray spikes by a standard software routine (CSMA, Princeton Instruments, NJ).

Sedimentation Velocity Experiments. Sedimentation velocity experiments were performed on a Beckman Optima XLA (Beckman, Palo Alto, CA) ultracentrifuge equipped with absorbance optics. Ultracentrifugation runs were carried out on 2−5 μM (heme) protein solutions at 20 °C and 48000 rpm in 0.1 M phosphate buffer, pH 7.0. The values of the sedimentation coefficients have been corrected to water at 20 °C ($s_{20,w}$) using standard procedures.

Molecular Dynamics Simulations. Molecular dynamics computations were carried out with the program MOIL, version 6.0 (*16*), using the locally enhanced sampling algorithm. This employs multiple copies of the ligands, each of which experiences the forces developed by interaction with the protein, which feels the average of these forces. The cutoff radius for non-bonded interactions was 10 Å, and the 1−4 scaling factors were 2 for electrostatic and 8 for van der Waals interactions. All crystallographic water molecules were included and modeled as TIP3 (*17*). The initial coordinates were taken from the crystal structure (*10*) after addition of polar hydrogens and energy minimization. As a measure of accessibility of heme iron to ligands, the number of ligand atoms within 4 Å of the iron was counted at the end of each picosecond of simulation.

RESULTS

State of Association. The ultracentrifugation experiments have been carried out in parallel on the CO derivatives of the native protein and of the H69V mutant. The sedimentation patterns of the two proteins are superimposable and yield $s_{20,w}$ values of 2.5 and 2.6 S for the mutant and the native protein, respectively. The mutation, therefore, does not affect the state of association of HbI.

Spectroscopic Characterization. The spectroscopic characterization of the H69V mutant has been limited to the deoxy and carbon monoxy derivatives since the oxygen

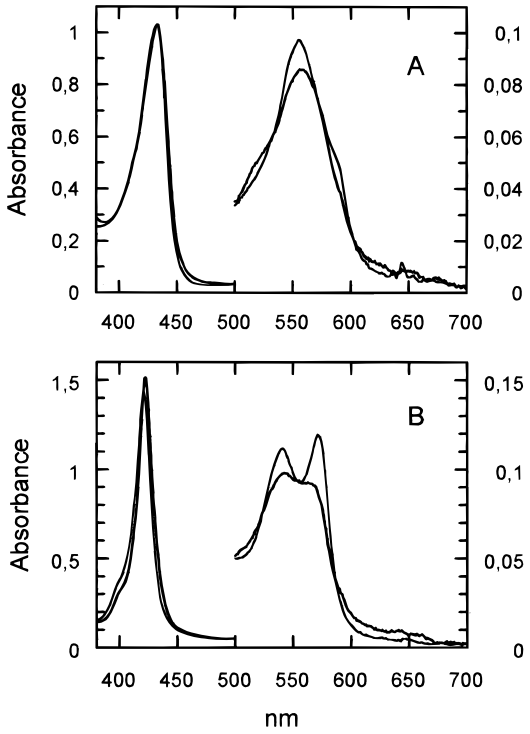

FIGURE 1: Absorption spectra of *Scapharca* HbI(H69V) (thick lines) and of the native protein (thin lines). (A) Deoxy derivatives. (B) Carbon monoxide derivatives. The spectra were measured in 0.1 M phosphate buffer at pH 7.0 and 20 °C. The protein concentration was 8×10^{-6} M; the optical path length was 1 cm.

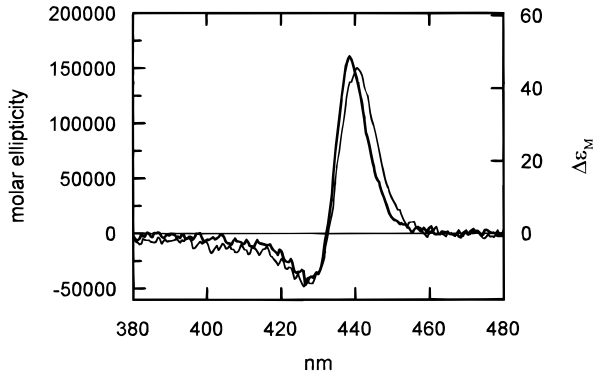

FIGURE 2: Circular dichroism spectra of *Scapharca* HbI(H69V) (thin line) and of the native protein (thick line). The spectra (deoxy derivative) were measured in 0.1 M phosphate buffer at pH 7.0 and 20 °C. The protein concentration was 8×10^{-6} M; the optical path length was 1 cm.

derivative is highly autoxidizable. Any attempt to study the oxygen binding properties, even in the presence of the enzymatic reducing system of Hayashi et al. (*18*), has been unsuccessful. The optical absorption spectra of the CO and deoxy H69V mutant are reported in Figure 1 in parallel with those of the native protein. In deoxygenated HbI(H69V) the intensity of the shoulder at 590 nm is markedly reduced with respect to the native protein. In the CO derivative the spectrum of the mutant is characterized by a higher ratio between the intensity of the $\beta(Q_1)$ band at 540 nm and that of the $\alpha(Q_0)$ band at 569 nm.

The circular dichroism spectra of deoxygenated H69V and native HbI in the Soret region are shown in Figure 2. The splitting in the deoxy Soret spectrum is similar in the native protein and in the mutant. This feature has been attributed to the interaction of the electric dipole transition moments (exciton splitting) of the two hemes (*19*) and therefore is diagnostic of their correct insertion in the heme pocket.

Resonance Raman spectra have been measured for the deoxy and CO derivatives of H69V and compared to the spectra measured previously on the native protein under similar conditions. The spectra of the deoxygenated proteins display significant differences. In the mutant the iron−His stretching peak occurs at a slightly lower frequency than in the native protein (199 as compared to 203 cm^{-1}) (Figure 3A). Other peaks in the low-frequency region, which have been shown to correlate with normal mode vibrations that receive a major contribution from the heme peripheral vibrational modes, are essentially unaltered in H69V with respect to the native protein, with the exception of the pyrrole bending sensitive lines at 757 and 787 cm^{-1} (Figure 3A). In fact, the relative intensities of these two lines are inverted in the mutant with respect to the native deoxy protein and closely match the intensities observed in the 10-ns CO photoproduct (*9*). In the high-frequency region of the resonance Raman spectrum most lines are the same in the mutant and in the native protein as expected for a ferrous high spin derivative (data not shown).

The resonance Raman spectra of the CO derivatives (Figure 4) have allowed the identification of the iron−carbon and carbon−oxygen stretching modes in the mutant. The frequencies of the modes involving the CO have been assigned through isotopic substitution with the double $^{13}C^{18}O$ isotope (Figure 4A). The value of 488 cm^{-1} (488/481 cm^{-1} for $^{12}C^{16}O$ /$^{13}C^{18}O$) assigned to the iron−carbon monoxide stretching mode is 30 cm^{-1} lower than that observed for the native protein. A similar effect has been observed in all distal His→apolar residues mutants in sperm whale myoglobin (*5*, *20*). As shown in Figure 4B, the C−O stretching mode is at 1945 cm^{-1} in the native protein (*21*), but it occurs at 1972 cm^{-1} (1972/1881 cm^{-1} for $^{12}C^{16}O$ /$^{13}C^{18}O$) in the H69V mutant. The Fe−C−O bending mode was observed to be very weak (572 cm^{-1}) and shifted to lower frequency compared to native HbI−CO which shows a bending mode at 582 cm^{-1} (Figure 4A).

CO Binding Kinetics. The mutant H69V (FeII) is rapidly oxidized by molecular oxygen, so only the reactions with CO could be studied. The binding reaction has been followed both by stopped flow, mixing deoxy protein with a solution of CO (Figure 5), and by flash photolysis, removing CO photochemically and following the recombination reaction. The rate of binding was the same in both kinds of experiment and, at 20 μM^{-1} s^{-1}, significantly faster than in the native protein. Further, the rate of CO rebinding following flash photolysis was independent of the fraction of CO removed, whereas in HbI showing cooperativity, the rate is higher at low fractional photolysis (*22*).

The amplitude and rate of nanosecond geminate recombination of CO are also notably different with an amplitude of some 60%, in contrast to native HbI and most hemoproteins, which typically show 3−5% geminate recombination (Figure 6). The observed rate constant for the geminate reaction in HbI (1.4×10^7 s^{-1}) is larger than that for the mutant (6×10^6 s^{-1}). Assuming that the rates and amplitudes of the geminate reactions express competition between ligand recombination and ligand escape from the immediate vicinity of the heme iron, the rates of the two

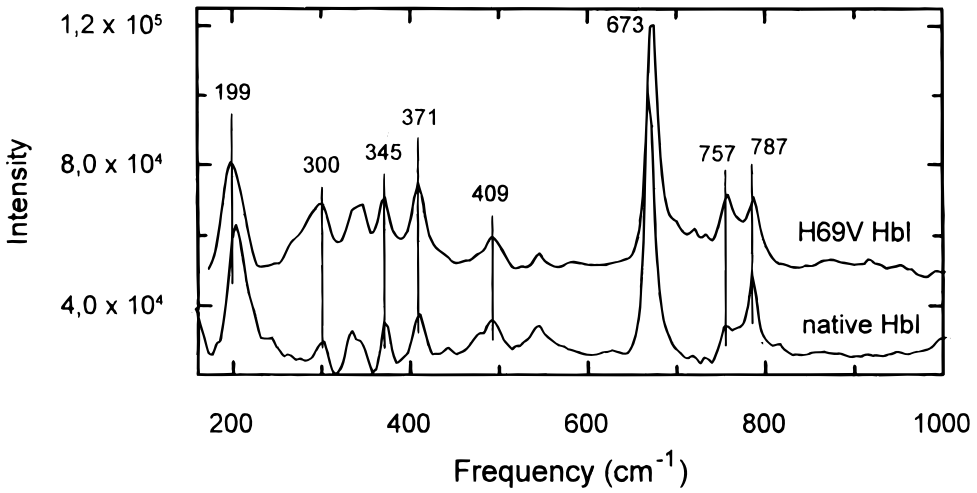

FIGURE 3: Resonance Raman spectra in the low-frequency region of the deoxy derivatives of *Scapharca* HbI(H69V) and of the native protein. Protein concentration was 50 μM in phosphate buffer at pH 7.0. The laser excitation wavelength was 441.6 nm.

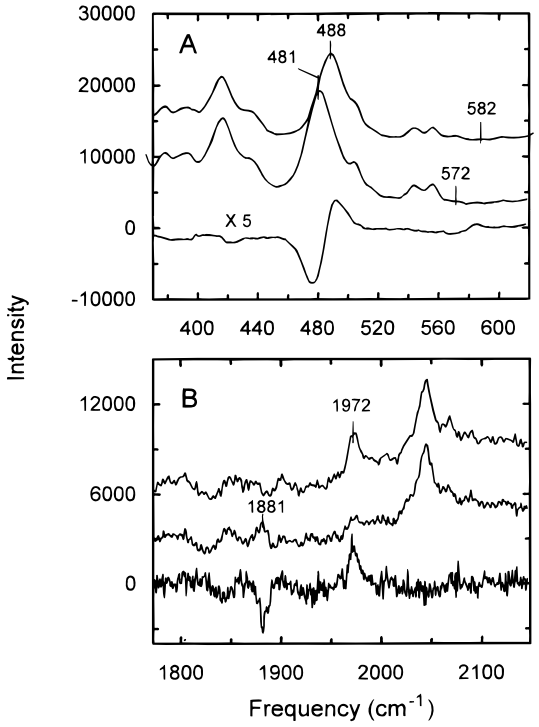

FIGURE 4: Isotopic dependence in the resonance Raman spectra of carbon monoxy *Scapharca* HbI(H69V). (A) Fe−CO stretching region. (B) C−O stretching region. From top to bottom: $^{12}C^{16}O$ derivative, $^{13}C^{18}O$ derivative, difference spectrum $^{12}C^{16}O - {}^{13}C^{18}O$. The protein concentration was 50 μM in phosphate buffer at pH 7.0. The laser excitation wavelength was 413 nm; the power at the sample was 1.5 mW.

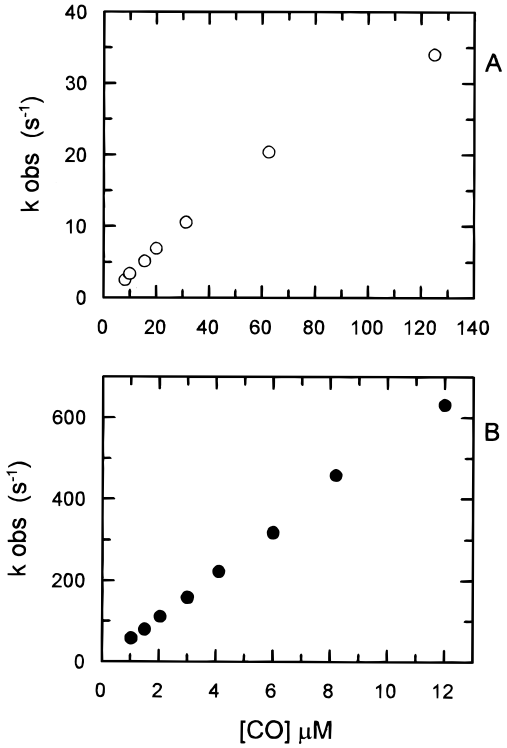

FIGURE 5: Pseudo-first-order plots for the reaction of carbon monoxide with native HbI (A) and with HbI(H69V) (B).

processes follow immediately. The rates of recapture by the iron are 0.07×10^7 and 0.41×10^7 for native and mutant, respectively, while the rates of escape are 1.4×10^7 and 0.25×10^7 s^{-1}. In other words, the specific rate of recapture is 6 times greater for the mutant, while the rate of escape is 5 times larger.

Molecular Dynamics Simulations. Simulations with native HbI are illustrated in Figure 7, and these can be compared to similar dynamics runs with the mutation H69V in Figure 8. The group of ligands in the locally enhanced sampling algorithm is held more tightly together and closer to the iron in the mutant than in native protein. In HbI, the ligands, as in many myoglobins, move quickly away from the iron in the first two or three picoseconds; in the mutant, they do not. In HbI, in as many as half of the runs, some ligands pass between Leu 36 and Ile 114 to a secondary location far from the heme iron. This has not been seen with the mutant, in which the number of close approaches to the iron atom is consistently high, scoring more than 80% of possible approaches. The behavior of the native protein is much more variable, with counts ranging from 20 to 60% in runs with different initial distributions of velocities. Small movements of the CD-E regions toward the heme may follow the mutation, and in one run the average distances between Val69 and the heme iron over 50 ps ranged between 8.74 and 9.35 Å compared with a range of 9.41 and 10.27 Å for the native protein. Similarly, the distances between Leu36 CG2 and

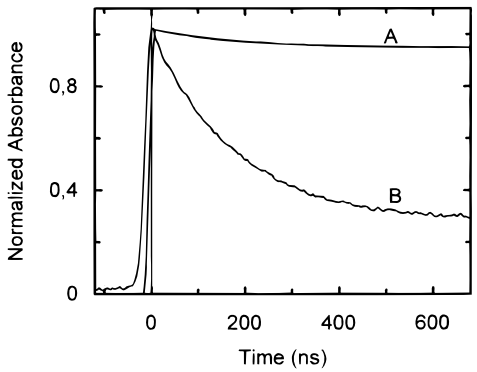

FIGURE 6: Time course of CO rebinding to native HbI (trace A) and to HbI(H69V) (trace B). The data for native HbI (taken from ref *32*) show about 5% geminate recombination. The mutant shows about 65% geminate recombination of 5 times longer duration with respect to the corresponding native HbI reaction. The wavelength was 435 nm; the flash duration was 9 ns.

Ile114 CD1 were 4.11 and 4.33 Å, and 5.11 and 5.08 Å for the mutant and native HbI, respectively.

DISCUSSION

The present study shows that in HbI the functional effects of the apolar mutation of the distal histidine His(69)→Val, and in particular the loss of cooperativity, can be correlated with specific changes in the heme geometry of the deoxygenated derivative.

The functional properties of the H69V mutant have been characterized in kinetic studies of the reaction with CO, due to the high rate of autoxidation of the mutated protein. The large increase in the second-order rate of CO binding (Figure 5) and the small change in the rate of ligand release relative to the native protein might be expected on the basis of the behavior of analogous mutants in several myoglobins (*2*). However, the change in the rate of CO binding to HbI(H69V) is unusually large (100-fold vs 10−20-fold in Mb). A further difference between the native protein and the H69V mutant is apparent upon partial photolysis of the CO derivative. In native HbI the increase in the CO rebinding rate upon partial photolysis is one of the kinetic manifestations of cooperativity (*22*). The lack of such an effect in the H69V mutant points to the absence of cooperativity.

The ligand binding behavior of H69V may be described in terms of a two-state allosteric scheme, coupled with the effects of substituting apolar residues for HisE7 in sperm whale myoglobin (*23*). Royer and collaborators (*24*, *25*) have shown that the ligand binding behavior of several mutants of HbI, and of HbI itself, may be described with a single set of kinetic parameters if it is supposed that singly liganded native HbI is predominantly in the T-state and that the doubly liganded form is divided between R and T. In high-affinity mutants, both singly and doubly liganded species are predominantly R-state, and even the unliganded form may have an R-state population sufficient to modify ligand binding significantly, even in stopped-flow experiments. For example, HbI(T72V) has an R-state CO binding rate of 7 μM^{-1} s^{-1} and a T-state rate 10 times smaller, compared to rates of 0.1 and 0.25 μM^{-1} s^{-1} in HbI for T and R, respectively. In this scheme, HbI(H69V) shows the largest binding rate so far observed for a mutant of HbI, about 3 times that for HbI(T72V) (*24*). This suggests that in HbI(H69V) the R-state itself has been modified by a direct effect of the nonpolar substitution on the ligand access to the heme. The required effect in HbI is less than in sperm whale Mb, where Quillin et al. (*23*) reported increases of 10-fold or more for analogous substitutions. Their increased rates may be attributed to relief of steric restraints close to the heme, coupled with partial breakdown of the histidine gate, leading to very high rates of oxygen dissociation from the sperm whale mutants. In this connection it is of interest that in βE7Phe, the only apolar mutant of HbA studied, the intrinsic ligand binding parameters are altered only slightly with respect to natural HbA since the effect of the mutation can be entirely accounted for in terms of a stabilization of the R-state (*6*, *26*). In turn, the behavior of the HbA−βE7Phe mutant is in accordance with the suggestion that the distal pocket in liganded β subunits is more open than in myoglobin (*27*).

The nature of the structural changes in the H69V HbI which lead to the stabilization of an R-like conformation are brought out clearly by the distinctive spectroscopic features of the deoxy derivative. In the optical absorption spectrum the shoulder at 590 nm is marked in native HbI, but it is almost completely abolished in the mutant (Figure 1). The presence of the 590-nm shoulder depends on the symmetry of the nuclear frame of the macrocycle and is correlated in particular with the departure from the C_4v symmetry that is typical of square pyramidal pentacoordinate complexes. On the basis of theoretical estimates and of the spectra of model compounds (*28*), the 590-nm shoulder has been assigned to a 0−0 (Q_0) electronic transition which is absent in the C_4v symmetry given the "electronically forbidden" character of the visible spectrum (*29*). Thus, the presence of an unusually high Q_0 band in native HbI indicates a distortion of the square pyramidal symmetry (*19*), while its absence in the H69V mutant points to a relatively more symmetric heme geometry. It should be pointed out that the H69V mutation does not affect the relative position of the two hemes since exciton splitting as apparent from the CD spectra (Figure 2) is unaltered with respect to the native protein.

The H69V mutation also induces slight shifts in the frequencies of some Raman modes of the deoxygenated derivative which have been proven to be reliable markers for the ligand-linked conformational transition in native HbI (*9*). The low frequency of the Fe−His stretching mode (203 cm^{-1}) in the native ligand-free deoxy HbI could be due to weakening of the Fe−His bond caused by steric strain exerted by the aromatic ring of Phe97 packing against the proximal histidine (*21*). A further downshift of this mode in the mutant suggests that Phe97 may have moved even closer to the proximal group. Changes in the spectrum of H69V with respect to native HbI are observed in the 740−790-cm^{-1} region, which has been reported to be sensitive to a symmetric pyrrole deformation mode (υ_{16}). Interestingly, the peaks at 757 and 787 cm^{-1} are essentially at the same positions in both the native protein and the mutant. However, the 757-cm^{-1} peak displays an enhanced intensity. The changes characterizing the H69V mutant with respect to native deoxy HbI are very similar to those observed in the 10-ns CO photoproduct and may likewise be interpreted in terms of an "R-like" conformation of the deoxy heme (*9*). However, the Fe−His stretching frequency is shifted to 199 cm^{-1} in the mutant (203 cm^{-1} in the native deoxy; Figure

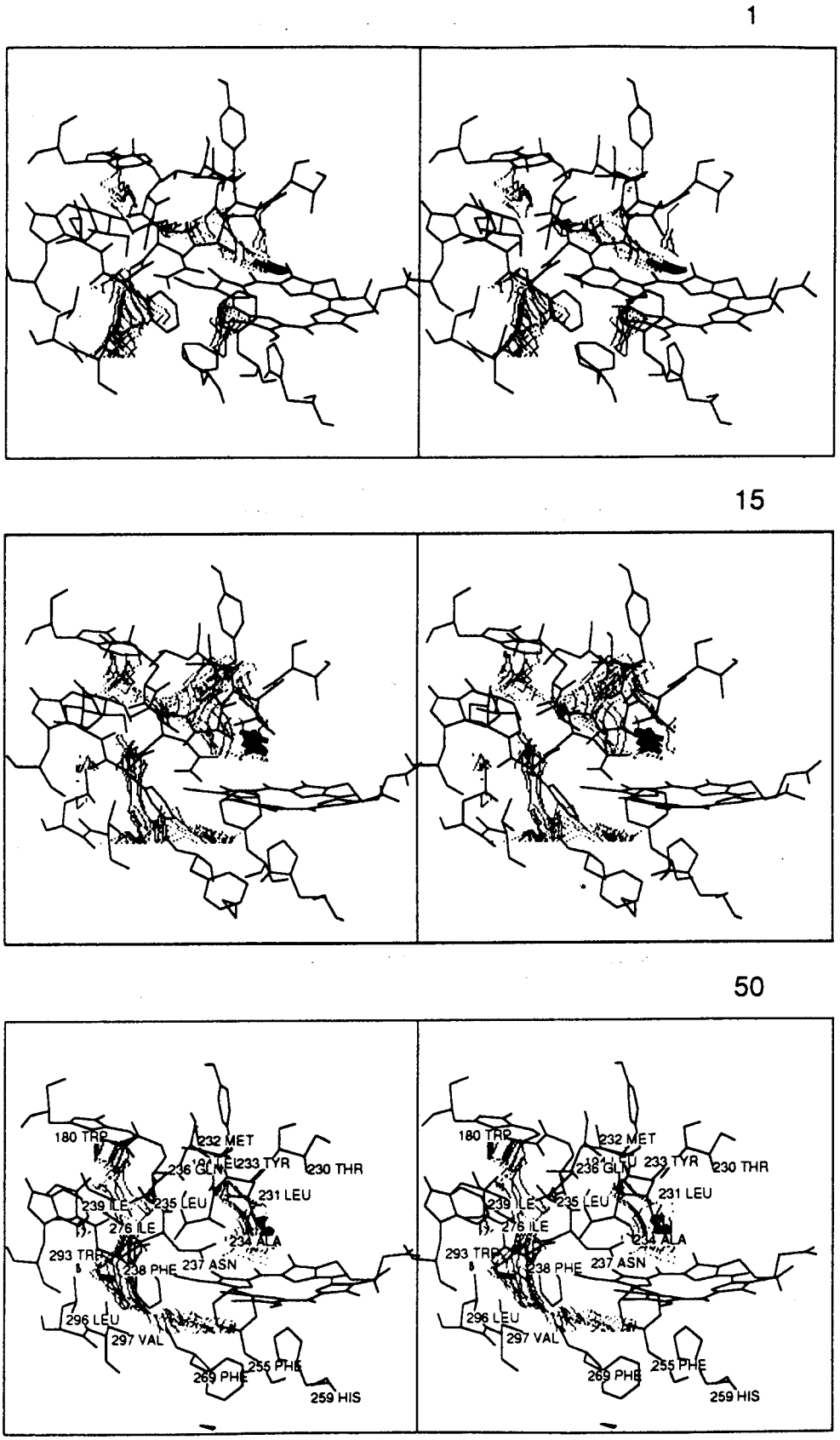

FIGURE 7: Molecular dynamics simulations of ligand diffusion in native *Scapharca* HbI. In the stereo frames the positions of ligand molecules (10 copies were used in the locally enhanced sampling algorithm) are shown as heavy solid bars. The light dots define the contours of spaces within the protein potentially able to accommodate a ligand molecule. The contour search volume was 12 Å^3 in all cases. Note that in the native protein the ligand group has moved further away from the iron atom than in the mutant (shown in Figure 8), and that in the later stages of the simulation ligands have moved to a secondary cavity to the left of the heme group. The time in picoseconds is shown above each frame.

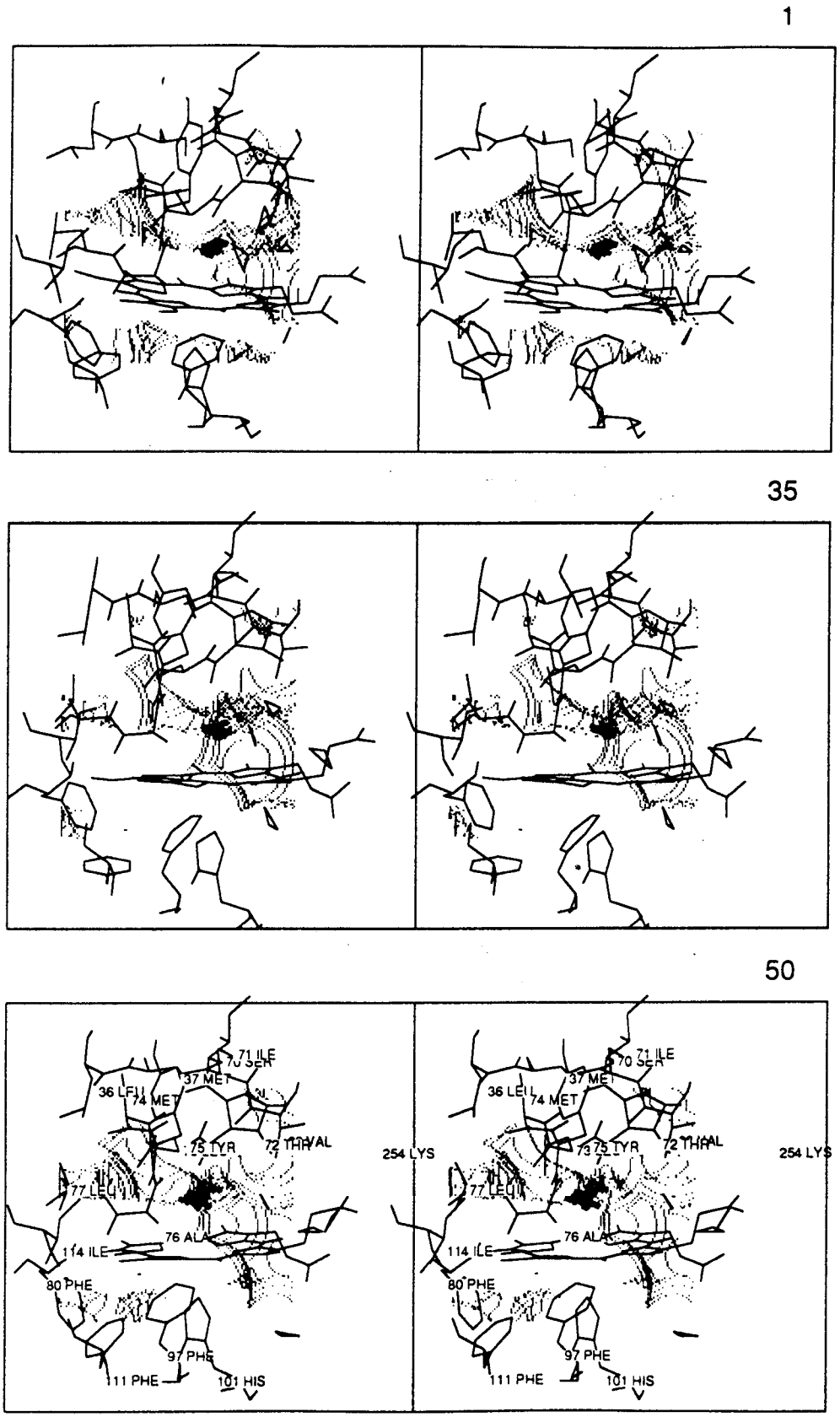

FIGURE 8: Molecular dynamics simulations of ligand diffusion in *Scapharca* H69V mutant. Molecular dynamics calculations were carried out as in Figure 7.

3) but occurs at 206 cm^{-1} in the 10-ns photoproduct (deoxy R conformation). The change in the proximal bond frequency in the mutant may reflect a change in the symmetry of the axial bond and may be related to the observed changes in the Q_0 band intensity (Figure 1). This is additional evidence that the communication pathway between the subunits does not occur along this coordinate, in contrast to mammalian hemoglobins (*9*, *11*). The changes observed in

the photolysis experiment are therefore interpreted as local tertiary changes associated with the ligand dissociation event.

The resonance Raman spectra of CO-bound HbI(H69V) indicate that the ligand binding geometry is altered as in analogous Mb mutants (*3*−*5*). In the mutant a ∼30 cm^{-1} decrease in the iron−carbon stretching frequencies and a similar increase in the diatomic ligand stretching frequencies are observed relative to the native protein (Figure 4). In most heme proteins and model compounds the iron−carbon stretching frequency and the internal C−O stretching frequency are inversely correlated (*30*). On this basis the frequencies characterizing the H69V mutant, taken together with the low intensity of the Fe−C−O bending mode, point to a CO molecule bound in a linear fashion as expected from the absence of distal steric hindrance. In addition, the H69V data are consistent with the absence of any polar interactions affecting the C−O associated frequencies as reported in an extensive study on Mb mutants with varying overall polarity of the distal pocket (*3*).

The structural differences in the heme symmetry of the H69V mutant with respect to the native protein revealed by the optical absorption and the resonance Raman spectra can thus be correlated with the stabilization of an R-like structure and are proposed here as the major cause for the lack of cooperativity. The diffusion of ligands in and around the heme pocket has been approached by molecular dynamics simulations, which have shown good correlation between computed ligand diffusion and ultrarapid ligand recombination in Mb mutants (e.g., ref *31*). In the case of HbI(H69V), no crystal structure is available to use as a starting point for computation, but high-resolution structures of a number of Mb mutants have shown little change other than that due to the substitution itself (*23*), suggesting that construction of a mutant molecule from the native coordinates is likely to give a good approximation to its structure. With this qualification, the results of MD are consistent with a role for steric changes in the distal pocket and with the increased amplitude and rate of geminate recombination of CO. In fact, as depicted in Figures 7 and 8, the average residence times of ligand molecules in the pocket are significantly increased when the distal His is replaced by Val.

In conclusion, the present study provides the first clear evidence that an apolar mutation of the distal histidine in a hemoglobin can have structural consequences on the proximal heme coordination geometry which leads to the stabilization of an R-like structure. It would be of great interest to establish whether a similar structural change underlies the stabilization of the R-like conformation of analogous HbA mutants or whether it is related to the unique structural coupling of the hemes in HbI.

REFERENCES

1. Springer, B. A., Sligar, S. G., Olson, J. S., and Phillips, G. N. (1994) *Chem. Rev. 94*, 699−714.
2. Rohlfs, R. J., Matthews, A. J., Carver, T. E., Olson, J. S., Springer, B. A., Egeberg, K. D., and Sligar, S. G. (1990) *J. Biol. Chem. 265*, 3168−3176.
3. Li, T., Quillin, M. L., Phillips, G. N., Jr., and Olson, J. (1994) *Biochemistry 33*, 1433−1446.
4. Morikis, D., Champion, P. M., Springer, B. A., and Sligar, S. G. (1989) *Biochemistry 28*, 4791−4800.
5. Anderton, C. L., Hester, R. E., and Moore, J. N. (1995) *Biochim. Biophys. Acta 1253*, 1−4.
6. Mathews, A. J., Rohlfs, R. J., Olson, J. S., Tame, J., Renaud, J. P., and Nagai, K. (1989) *J. Biol. Chem. 264*, 16573−16583.
7. Chiancone, E., Verzili, D., Boffi, A., Royer, W. E., Jr., and Hendrickson, W. A. (1990) *Biophys. Chem. 265*, 4828−4831.
8. Royer, W. E., Jr., Hendrickson, W. A., and Chiancone, E. (1990) *Science 249*, 518−524.
9. Rousseau, D. L., Song, S., Friedman, J. M., Boffi, A., and Chiancone, E. (1993) *J. Biol. Chem. 268*, 5719−5723.
10. Royer, W. E., Jr. (1994) *J. Mol. Biol. 235*, 657−681.
11. Coletta, M., Boffi, A., Ascenzi, P., Brunori, M., and Chiancone, E. (1990) *J. Biol. Chem. 265*, 4828−4830.
12. Sambrook, J., Fritsch, E. F., and Maniatis, T. (1989) in *Molecular Cloning: A Laboratory Manual*, Cold Spring Harbor Laboratory Press, Cold Spring Harbor, NY.
13. Summerford, C. N., Pardanani, A., Betts, A. H., Poteete, A. R., Colotti, G., and Royer, W. E., Jr. (1995) *Protein Eng. 8*, 593−599.
14. Sharma, V. S., Ranney, H. M., Geibel, J. F., and Traylor, T. G. (1975) *Biochem. Biophys. Res. Commun. 66*, 1301−1306.
15. Koechner, W. (1988) in *Solid State Laser Engineering*, p 301, Springer Press, Berlin.
16. Elber, R., Roitberg, A., Verkhiver, G., Goldstein, R., Li, H., and Simmerling, C. (1993) in *MOIL: A Molecular Dynamics Program with Emphasis on Reaction Path Calculations and Conformational Searches in Proteins in Advances in Computational Biology* (Villary, H., Ed.) Jai Press Inc., Greenwich, CT.
17. Jorgensen, W. L., and Tirado-Rives, J. (1988) *J. Am. Chem. Soc. 110*, 1657−1666.
18. Hayashi, A., Suzuki, T., and Shin, M. (1973) *Biochim. Biophys. Acta 310*, 309−316.
19. Chiancone, E., Vecchini, P., Verzili, D., Ascoli, F., & Antonini, E. (1981) *J. Mol. Biol. 152*, 577−592.
20. Ling, J., Li, T., Olson, J. S., and Bocian, D. F. (1994) *Biochim. Biophys. Acta 1188*, 417−421.
21. Song, S., Boffi, A., Chiancone, E., and Rousseau, D. L. (1993) *Biochemistry 32*, 6330−6336.
22. Antonini, E., Ascoli, F., Brunori, M., Chiancone, E., Verzili, D., Morris, R. J., and Gibson, Q. H. (1984*) J. Biol. Chem. 259*, 6730−6738.
23. Quillin, M. L., Arduini, R. M., Olson, J. S., and Phillips, G. N., Jr. (1993) *J. Mol. Biol. 234*, 140−155.
24. Royer, W. E., Jr., Pardanani, A., Gibson, Q. H., Peterson, E. S., and Friedman, J. M. (1996) *Proc. Natl. Acad. Sci. U.S.A.* 93, 14526−14531.
25. Pardanani, A., Gibson, Q. H., Colotti, G., and Royer, W. E., Jr. (1997) *J. Biol. Chem. 272*, 20, 13171−13179.
26. Kiger, L., Baudin, V., Deesbois, A., Pagnier, J., Kister, J., Griffon, N., Henry, Y., Poyart, C., and Marden, M. C. (1997) *Eur. J. Biochem. 243*, 365−373.
27. Shaanan, B. (1983) *J. Mol. Biol. 171*, 31−50.
28. Wang, C. M., and Brinigar, W. S. (1979) *Biochemistry 18*, 4960−4977.
29. Eaton, W. E., and Hofrichter, J. (1976) *Methods Enzymol. 76*, 175−225.
30. Yu, N. T., Kerr, A., Ward, B., and Chang, C. K. (1983) *Biochemistry 22*, 4534−4539.
31. Gibson, Q. H., Regan, R., Elber, R., Olson, J. S., and Carver, T. E. (1992) *J. Biol. Chem. 267*, 22022−22034.
32. Chiancone, E., Elber, R., Royer, W. E., Jr., Regan, R., and Gibson, Q. H. (1993) *J. Biol. Chem. 268*, 5711−5718.

BI972380F